An Endocytosed TGN38 Chimeric Protein Is Delivered to the TGN after Trafficking through the Endocytic Recycling Compartment in CHO Cells

Richik N. Ghosh, William G. Mallet, Thwe T. Soe, Timothy E. McGraw, and Frederick R. Maxfield

Department of Biochemistry, Cornell University Medical College, New York, New York 10021

Abstract. To examine TGN38 trafficking from the cell surface to the TGN, CHO cells were stably transfected with a chimeric transmembrane protein, TacTGN38. We used fluorescent and ^{125}I-labeled anti-Tac IgG and Fab fragments to follow TacTGN38's postendocytic trafficking. At steady-state, anti-Tac was mainly in the TGN, but shortly after endocytosis it was predominantly in early endosomes. 11% of cellular TacTGN38 is on the plasma membrane. Kinetic analysis of trafficking of antibodies bound to TacTGN38 showed that after short endocytic pulses, 80% of internalized anti-Tac returned to the cell surface ($t_{1/2}$ = 9 min), and the remainder trafficked to the TGN. When longer filling pulses and chases were used to load anti-Tac into the TGN, it returned to the cell surface with a $t_{1/2}$ of 46 min. Quantitative confocal microscopy analysis also showed that fluorescent anti-Tac fills the TGN with a 46-min $t_{1/2}$. Using the measured rate constants in a simple kinetic model, we predict that 82% of TacTGN38 is in the TGN, and 7% is in endosomes. TacTGN38 leaves the TGN slowly, which accounts for its steady-state distribution despite the inefficient targeting from the cell surface to the TGN.

Key words: *trans*-Golgi network • endocytosis • endosome • protein sorting

INTEGRAL membrane proteins and macromolecules that are endocytosed at the cell surface can have several intracellular fates (12, 34). The major endocytic trafficking pathways deliver recycling receptors back to the plasma membrane via the early endosomal system, and transport soluble volume markers to late endosomes and lysosomes (12, 34). Several endocytosed integral membrane proteins can have other destinations. For example, cation-independent mannose-6-phosphate receptors (CI-M6PR) traffic from the cell surface to late endosomes (22), and a significant fraction of endocytosed EGF receptors are targeted for degradation (8, 25). It has long been recognized that some endocytosed membrane proteins are delivered to the TGN (7, 11, 17, 43). For many proteins this delivery may represent missorting, but some proteins are selectively targeted to the TGN after endocytosis. Furin (33) and TGN38 (1, 40, 44) are two examples of such proteins. Peptide sequences responsible for targeting these proteins to the TGN have been characterized (3, 4, 15, 21, 37, 47, 49).

At steady-state a small fraction of TGN38 is at the cell surface, and this surface pool undergoes dynamic exchange with intracellular TGN38, which is mainly in the TGN (1, 23, 24, 40). The distribution of TGN38 implies rapid internalization and delivery to the TGN coupled with slower exit and return to the plasma membrane. The intracellular itinerary followed by TGN38 is not known, but two routes for delivery from early endosomes to the TGN seem most plausible. One route would go from early sorting endosomes to late endosomes, and then to the TGN. This route has been proposed as the itinerary followed by CI-M6PR after endocytosis, and there is evidence that a fraction of most endocytosed proteins follow this route (11). The second route would go from the sorting endosomes to the endocytic recycling compartment (ERC),[1] and from there to the TGN. There is no direct evidence for trafficking from the ERC to the TGN in mammalian cells, but these compart-

The first two authors contributed equally to this work.

Address all correspondence to Dr. F.R. Maxfield, Department of Biochemistry, Cornell University Medical College, New York, NY 10021. Tel.: 212-746-6405. Fax: 212-746-8875. E-mail: frmaxfie@mail.med.cornell.edu

1. *Abbreviations used in this paper*: ERC, endocytic recycling compartment; F-anti-Tac, fluorescein-conjugated anti-Tac antibody; F-IgG, fluorescein-conjugated IgG; F-Tf, fluorescein-conjugated transferrin; F-dex, fluorescein-conjugated dextran; M6PR, mannose-6-phosphate receptor; C_6-NBD-ceramide, *N*-(ϵ-7-nitrobenz-2-oxa-1,3-diazol-4-yl-aminocaproyl)-D-erythro-sphingosine; R-dex, rhodamine-conjugated dextran; Tf, human transferrin; TR, transferrin receptor.

ments are frequently in close proximity (18, 51). Furthermore, it has recently been shown that they both have rab11 associated with their membranes (45, 46), and in some brefeldin A—treated cells the ERC and the TGN become fused (26, 51). A recent report suggests that in yeast, the protease Kex2p trafficks to the TGN via early, not late endosomes (13). These results suggest that there may be direct membrane traffic between the ERC and the TGN.

To follow the pathway taken from the cell surface to the TGN we used a chimeric transmembrane protein, TacTGN38, which has the lumenal domain of the IL-2 receptor alpha chain (Tac) and the cytoplasmic and transmembrane domains of TGN38 (15). TacTGN38 has been shown to localize to the TGN in several different cell types (15, 39). For our studies, TacTGN38 was stably expressed in cells of the CHO-derived line TRVb1, which lacks the native hamster transferrin receptor but stably expresses the human transferrin receptor (TR; 30). This expression allowed us to use human transferrin as a marker for the endocytic recycling pathway, and anti-Tac monoclonal antibodies as a marker for the pathway to the TGN. We found that nearly all internalized TacTGN38 trafficks through the ERC, and most of it recycles back to the cell surface. During each round of endocytosis ~20% of TacTGN38 is retained in the cell, and this retained TacTGN38 is delivered to the TGN. We did not detect significant amounts of TacTGN38 accumulating in late endosomes. The exit from the TGN was slow, accounting for the predominant steady state distribution in the TGN.

Materials and Methods

Cell Lines

TRVb1 cells, a CHO cell line lacking the endogenous TR and stably expressing the human TR (30), were grown in either Ham's F12 or McCoy's 5A medium containing 5% FBS, penicillin-streptomycin, 220 mM sodium bicarbonate, and 400 μg/ml G418. The cells were grown at 37°C in a humidified atmosphere of 5% CO_2. The TacTGN38 chimera was the kind gift of J. Bonifacino (National Institutes of Health, Bethesda, MD), and consists of the lumenal domain of the T cell antigen Tac and the cytoplasmic and transmembrane domains of TGN38 (15, 39). The TacTGN38 chimera was transfected into TRVb1 cells with the hygromycin-resistant plasmid pMEP using Lipofectin (GIBCO BRL, Gaithersburg, MD). These doubly transfected cells were selected in 400 μg/ml G418 and 420 U/ml hygromycin. To isolate clonal lines stably expressing TacTGN38, these cells were first incubated with Cy3 labeled anti-Tac IgG at 37°C for 60–120 min to allow significant uptake and labeling of the TacTGN38 in the TGN, and then FACS was used to isolate single cells. Unless otherwise indicated, all data were derived from a single clone.

Antibodies

Monoclonal anti-Tac antibodies (isoform IgG1) were obtained from the mouse hybridoma cell line 2A3A1H (American Type Culture Collection, Rockville, MD). These cells were grown in protein-free hybridoma media (GIBCO BRL), and the anti-Tac IgG was isolated using a Sephacryl S-300 gel filtration column and FPLC. Fab fragments were generated using papain in a Fab preparation kit (Pierce Chemical Co., Rockford, IL), and were further purified by a Protein A column and FPLC. Rabbit polyclonal antibodies against the cytoplasmic domain of TGN38 (27) were a gift of Dr. Keith Stanley (Heart Research Institute, Sydney, Australia). Rabbit polyclonal antibodies against the lumenal domain of furin (32) were a gift of Dr. Yukio Ikehara (Fukuoka University School of Medicine, Japan).

Ligands

Human transferrin (Tf) was purchased from Sigma Chemical Co. (St. Louis, MO), purified by Sephacryl S-300 gel filtration, and iron-loaded as previously described (51). Cy3 and Alexa488 were conjugated to Tf, anti-Tac IgG, or anti-Tac Fab according to the manufacturer's instructions (Biological Detection Systems, Pittsburgh, PA, or Molecular Probes Inc., Eugene, OR, respectively). IgG was labeled with ^{125}I according to our earlier protocol (51). Fluorescein labeling of Tf or IgG was done as previously described (51). *N*-(ε-7-nitrobenz-2-oxa-1,3-diazol-4-yl-aminocaproyl)-D-erythro-sphingosine (C_6-NBD-ceramide), 70 kD fluorescein or rhodamine-labeled, fixable dextran, and antifluorescein antibodies were purchased from Molecular Probes, Inc. (Eugene, OR). Fluorescent anti-mouse or anti-rabbit IgG antibodies were purchased from either Pierce Chemical Co. or Cappel Laboratories (Malvern, PA).

Accumulation of [^{125}I]Anti-Tac Antibody in Cells

Duplicate 35-mm wells of confluent TRVb1/TacTGN38 cells were incubated for different times at 37°C in the continuous presence of 10^6 cpm per well of [^{125}I]anti-Tac antibody in McCoy's 5A medium with 1% (wt/vol) BSA (final IgG concentration of 10 μg/ml). At the end of the incubation, cells were washed extensively with ice-cold Medium 1 (150 mM NaCl, 20 mM Hepes, 1 mM $CaCl_2$, 5 mM KCl, 1 mM $MgCl_2$, pH 7.4) with 1% (wt/vol) BSA, and were solubilized in 0.1% (wt/vol) SDS in 0.1 M NaOH. Solubilized radioactivity was determined using a gamma counter. Nonspecific counts were determined by incubation of cell-free wells with [^{125}I]anti-Tac antibody, and were subtracted from the counts extracted from cells.

To determine the proportion of TacTGN38 on the plasma membrane, cells were washed with ice-cold McCoy's 5A medium with 1% (wt/vol) BSA and allowed to cool on ice for 30 min. Cells then were incubated with [^{125}I]anti-Tac IgG at 0°C for 30 min, and were washed with Medium 1/BSA and solubilized as described above. Absence of antibody internalization at 0°C was confirmed by microscopy using a fluorescently labeled anti-Tac antibody.

Internalization Rate Constant Determination

The TacTGN38 internalization rate constant (k_i) was derived from plots of the internal/surface ratio at different times, as described previously (31, 48). Cells were cultured to confluence in 24-well plates. Triplicate wells of TacTGN38-transfected cells were incubated with 0.5 ml ^{125}I-labeled anti-Tac IgG (4 μg/ml, 10^7 cpm/well) from 1 to 5 min at 37°C. To determine nonspecific binding, single wells of TRVb1 cells not transfected with TacTGN38 were incubated with IgG over the same time course. After incubations, cells were placed into a 4°C ice bath and washed rapidly with prechilled 4× 1 ml Medium 1 + 1% (wt/vol) BSA, and then with 1 ml Medium 1. Surface-bound IgG was eluted with 2× 1-ml washes of 0.1 M acetic acid, 0.5 M NaCl; 10 min each wash at 0°C. This procedure eluted ~98% of all surface-bound counts, as determined from control samples that were incubated with IgG at 4°C to prevent internalization. After the elutions, cells were washed with 1 ml Medium 1 and solubilized by 2× 1 ml incubations with 0.1 M NaOH, 0.1% (wt/vol) SDS at 37°C, 15 min each incubation. Surface and internal counts were obtained using a gamma counter. The counts were corrected for nonspecific binding and the efficiency of the low pH elution, and then the internal-to-surface ratio was calculated for each sample. The ratios were plotted as a function of time, and the slope of the line (k_i) was calculated by linear regression (see Fig. 2 *b*).

Fluorescence Staining Methods

For fluorescence microscopy, TRVb1/TacTGN38 cells were grown to subconfluence on poly-D-lysine–treated coverslips affixed to holes cut in the bottoms of tissue culture dishes. Unless otherwise stated, cells were incubated with fluorescent probes, washed, and subjected to chases in McCoy's 5A medium (GIBCO BRL) supplemented with 2.2 g/liter $NaHCO_3$, 20 mM Hepes, and 0.2% (wt/vol) BSA (Sigma Chemical Co.) at 37°C. For brief incubations and washes, cells were placed on a 37°C slide warmer. For longer intervals, cells were placed in a 37°C incubator under an atmosphere of 5% CO_2. Immediately before fixation, cells were washed rapidly with Medium 1 at room temperature. Cells were fixed with 4% paraformaldehyde in Medium 1 for 10 min at room temperature. After fixation, cells were rinsed with Medium 1 with the addition of 10 mM methylamine to disperse intracellular pH gradients. To stain the TGN with C_6-NBD-ceramide, the cells were first fixed and then incubated with 5 mM C_6-NBD-ceramide in Medium 1 for 30 min at room temperature. The cells were then washed four times (15 min for each wash) in Medium 1 containing 25 mg/ml fatty-acid free BSA.

Microscopy

Fluorescence microscopy was done either on a DMIRB inverted microscope (Leica Inc., Deerfield, IL) using a 63× 1.32 NA plan Apochromat objective, or an MRC600 laser scanning confocal unit attached to an Axiovert microscope (Carl Zeiss Inc., Thornwood, NY) with a 63× 1.4 NA plan Apochromat objective (Leica Inc.). The excitation on the Leica microscope was by a Hg arc 100W lamp (Leica Inc.) with standard fluorescein and rhodamine optics. Images were taken with one of two different cooled CCD cameras from Princeton Instruments (Trenton, NJ): either a TEA CCD K1317 camera with a KAF-1400 Kodak 1317 × 1075 chip, or a Pentamax 512EFTB frame transfer camera with a 512 × 512 back-thinned EEV chip. The laser on the confocal microscope was a 25 mW Argon ion laser emitting at 488 nm and 514 nm. The confocal microscope was calibrated as described before (9, 10).

C_6NBD-Ceramide Imaging

NBD has a broad emission spectrum that leaks through the filters used to select Cy3's emission on the confocal microscope; conversely, the Cy3 emission does not leak into the detector meant for green (NBD) fluorescence. To ensure no emission fluorescence was imaged by the wrong detector, the following confocal microscopy protocol was used to image cells that were doubly labeled with C_6-NBD-ceramide and Cy3-IgG or Cy3-Tf. First, a single focal plane image of the C_6NBD-ceramide was obtained by exciting the sample at 488 nm and imaging with the filters and detector used for green fluorescence. Then, the NBD was further illuminated at 488 nm to photobleach it. NBD is extremely photolabile and photobleaches rapidly, whereas Cy3 is much more resistant to photobleaching. The amount of light used to photobleach NBD does not significantly affect Cy3's fluorescence. An image was then taken of the Cy3 distribution by exciting the sample at 514 nm and imaging with the filters and detector used for red fluorescence. This Cy3 image now contains no contaminating NBD fluorescence.

Image Processing and Quantification

Image processing was done using the MetaMorph image processing package (Universal Imaging Corp., West Chester, PA) on a Pentium PC. To analyze the amount of Cy3 fluorescence per labeled TGN (see Figs. 9 and 10), first a local median background intensity obtained from a 32 × 32 pixel area (0.15 μm/pixel) was subtracted from every pixel of the Cy3 and NBD images, as previously described (6). A mask to identify the TGN was then obtained by retaining those pixels whose intensities in the NBD image were above a specific threshold value. The threshold value was the mean plus 3 standard deviations of all the positive pixels intensities in the NBD image. To complete the mask, these retained pixels were all given the same constant intensity, and the rest of the image was made black. This mask delineates the areas of bright NBD labeling from the dimmer, background, and cellular haze (see Fig. 9, *c* and *e*). The selected region was robust to the intensity threshold value chosen, as a lower threshold of the mean intensity plus two standard deviations gave similar results. This mask was applied to the Cy3 image (see Fig. 9 *d*), and the intensities in only those Cy3 pixels that were in the area delineated by the mask (see Fig. 9 *f*) were summed. This summed intensity was normalized by the number of pixels in the mask, giving the Cy3 intensity per TGN element (pixel).

In the experiments where the entire 3-D fluorophore distributions were imaged by confocal microscopy, the samples were brightly labeled, allowing the excitation light to be reduced; hence, the samples were not photobleached. In addition, cross-talk of the fluorophores into the wrong detectors was also negligible. To quantify these images, first each slice had its local (30 × 32 pixel area) median background subtracted. Then, the out-of-focus background in each Cy3 slice was corrected by a nearest-neighbor deblurring procedure where the scaled average of the intensities in the two adjacent slices was subtracted from the current slice. This procedure sharply emphasized the TGN staining in the current slice, and deemphasized out-of-focus haze from staining in the other slices. This Cy3 image was then thresholded (mean + 3 SD), and the resulting mask delineating the area covered by the TGN was applied to the corresponding fluorescein green image. The thresholded intensities of the green pixels that were selected by the mask were summed for each slice (the green threshold was mean + 1 SD; this selects the cell-associated fluorescein fluorescence, but rejects any noncell background). The intensities from the selected green pixels were summed over all slices in the 3-D stack, and were then normalized by the total number of pixels in all the TGN masks from every slice in the stack. This summation gave the fluorescein fluorescence per TGN volume element in Fig. 10 (*circles*).

To quantify the fluorescence from images in the fluorescein quenching experiments (see Figs. 6, 7, and 11), the background fluorescence was first subtracted from each image. This background was determined as the mean intensity from a cell-free region. The remaining cell-associated fluorescence was summed and divided by the number of cells in the field to derive the fluorescence power per cell. Ten fields of cells were imaged for each experimental condition or time point, typically with about twenty cells per field.

Fluorescence Quenching with HRP-Tf

HRP-Tf was made by first attaching the *N*-hydoxysuccinimide-ester-maleimide cross-linker sulfo-MBS (*m*-Maleimidobenzoyl-*N*-hydroxysuccinimide ester; Pierce Chemical Co.) to HRP (Sigma Chemical Co.), resulting in a maleimide group attached to the ϵ-amine of lysine by an amide bond. Specifically, 0.5 ml of 8.3 mg/ml of sulfo-MBS in PBS was added to 0.5 ml of 40 mg/ml HRP in PBS, incubated for 1 h at room temperature under argon gas, and then passed over a Sephadex G-25M PD-10 gel filtration column (Pharmacia Biotech Sverige, Uppsala, Sweden). A sulfhydryl residue was attached to the ϵ-amine of Tf's lysines by reacting diferric Tf (0.4 ml; 46 mg/ml) with the cyclic thioimidate 2-iminithiolane (IT; Traut's reagent; 0.1 ml of 32 mg/ml in PBS; Pierce Chemical Co.) by incubating them together for 40 min at room temperature under argon gas, and then passing them over a PD-10 column. The maleimide group on the HRP is reactive to the sulfhydryl group attached to Tf. The HRP-MBS and the Tf-IT were incubated together at room temperature for 4 h under argon. The reaction was quenched with 30 mg/ml pH 7.8 Tris buffer. The reaction mixture was concentrated and passed over a S-300 Sephacryl gel filtration column, and the fractions were assayed for protein concentration and purity.

In the HRP-Tf fluorescence quenching experiments, incubations and chases were done in McCoy's 5A medium supplemented with 2.2 g/liter $NaHCO_3$, 20 mM Hepes, and 0.2% (wt/vol) BSA (Sigma Chemical Co.) at 37°C. Cells were incubated with either 1 μg/ml Cy3 anti-Tac IgG for 10 min or with 5 μg/ml Cy3-Tf for 30 min, chased for 10 min with 50 μg/ml HRP-Tf, fixed with 4% paraformaldehyde and 80 mM methylamine in Medium 1 for 10 min at room temperature, and then treated with 0.0025% hydrogen peroxide and 25 μg/ml DAB before viewing on the microscope. In certain cases, 5 mg/ml of unlabeled Tf was included with the HRP-Tf in the chase media.

Detection of TacTGN38 in Late Endosomes

To label late endosomes, fixable 70-kD dextran conjugated to either rhodamine (R-dex) or fluorescein (F-dex; Molecular Probes, Inc.) was reconstituted to 50 mg/ml and dialyzed extensively against McCoy's 5A medium to remove free dye. TacTGN38 cells were incubated with 20 mg/ml F-dex, and with either 2 μg/ml Cy3-labeled anti-Tac IgG or 20 mg/ml R-dex in McCoy's medium with 0.1% (wt/vol) BSA for 10 min at 37°C. After incubations, cells were washed with McCoy's medium + 0.1% (wt/vol) BSA and chased for 20 min, and then fixed with paraformaldehyde. The cells were imaged by confocal microscopy. Individual confocal slices were corrected for background fluorescence and cross-talk before the F-dex and Cy3-IgG or R-dex colocalization was evaluated.

Results

Endocytosed Fluorescent Anti-Tac Antibodies Traffic to the TGN

TRVb1 cells were transfected with TacTGN38, and clonal cell lines were selected by FACS sorting using Cy3-labeled monoclonal anti-Tac IgG. We first examined the distribution of internalized Cy3-labeled anti-Tac IgG and monovalent Fab. Fig. 1 shows confocal microscopy images of Cy3-Fab (Fig. 1 *b*) and Cy3-IgG (Fig. 1 *d*) after a 5–10 min incubation with the antibodies and a 30–40-min chase. The cells were also stained with C_6-NBD-ceramide which labels the TGN (36), and single optical sections were obtained in regions that showed significant NBD fluorescence (Fig. 1, *a* and *b*). Both the IgG and the Fab showed

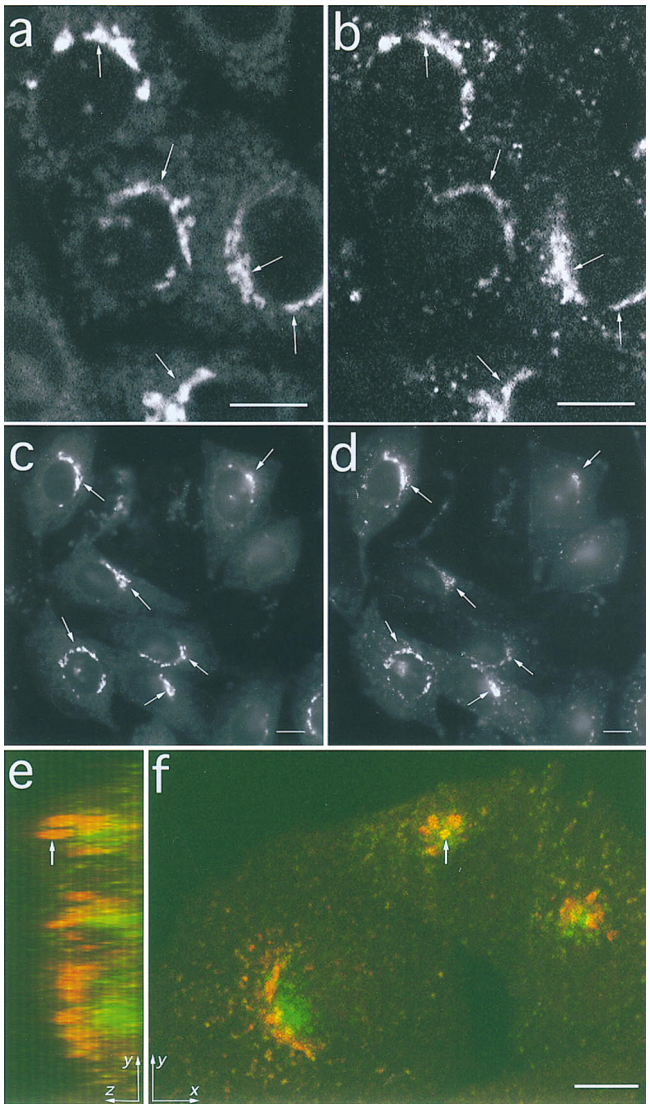

Figure 1. Endocytosed fluorescent anti-Tac antibodies traffic to the TGN. Cells were labeled with Cy3 conjugated anti-Tac Fab for 10 min at 37°C and then chased for 40 min. The cells were fixed and labeled with C_6-NBD-ceramide to identify the TGN. (*a*) A single confocal microscope section showing the C_6NBD-ceramide staining; (*b*) Cy3-Fab labeling. These images show that the endocytosed Fab reaches the TGN (*arrows*). (*c* and *d*) Images taken by wide-field microscopy of C_6-NBD-ceramide (*c*) and Cy3-IgG (*d*) show that endocytosed Cy3-IgG can also reach the TGN (*arrows*). (*e* and *f*) Cells were incubated with F-Tf at 37°C for 30 min to label the ERC (*green*), and then they were fixed, permeabilized, and labeled with Cy3-IgG to identify the TGN (*red*). A 3-D stack of images through the cell was obtained by confocal microscopy. (*f*) An x-y maximum projection of this stack, and (*e*) a y-z maximum projection of the same cells, which is similar to viewing the cells from the right-hand side. The arrow indicates that although a part of the TGN may appear colocalized with the ERC in an x-y projection (*f*), the y-z projection shows that it is in a different vertical position (e). In these cells the TGN is to the side and above the ERC. Bar, 10 μm.

extensive colocalization with the C_6-NBD-ceramide, demonstrating that the endocytosed Cy3 labeled anti-Tac Fab and IgG reached the TGN. After an extensive chase, internalized anti-Tac also codistributed with furin, an endoprotease that is localized to the TGN (see Fig. 4, *c* and *d*). Endocytosed TacTGN38 trafficked to the TGN in all the clonal lines we examined.

We also compared the distribution of endocytosed anti-Tac IgG with indirect immunofluorescence against TGN38 using an antibody against the cytoplasmic domain of TGN38 that recognizes both the endogenous TGN38 and the expressed TacTGN38. All elements that were labeled with anti-TGN38 also contained endocytosed anti-Tac (data not shown). Therefore, endocytosed anti-Tac does not label a subset of TacTGN38 that is distinct from the total pool of expressed protein. When cells were incubated with anti-Tac IgG and Fab together for 10 min and chased for an hour, the probes colocalized in a perinuclear structure resembling the TGN. We did not detect any difference in the distribution of internalized Fab as compared with the intact IgG (not shown). In TRVb1 cells that had not been transfected with TacTGN38, we did not detect observable binding or internalization of Cy3 anti-Tac Fab, demonstrating that antibody uptake required binding to TacTGN38 (not shown). Preparation of Fab fragments from mouse IgG1 results in low yields, so we elected to use intact anti-Tac IgG for most of the subsequent studies.

Endocytosed recycling receptors traffic through the early endosomal system which, in CHO cells, consists of punctate sorting endosomes and the tubulovesicular, juxtanuclear ERC (6, 12, 51). Although both the ERC and the TGN have a perinuclear location, we have previously shown that they are separate compartments (18). We demonstrate this further in Fig. 1, *e* and *f*, where cells were first incubated with fluorescein-conjugated transferrin (F-Tf) at 37°C for 30 min to label the ERC (*green*), and then were fixed, permeabilized, and labeled with Cy3-IgG to identify the TGN (*red*). The 3D distribution of these probes was obtained by confocal microscopy by acquiring a stack of images taken at successive focal planes through the cell. Fig. 1 *f* shows an x-y projection of this stack, where the maximum pixel intensity at each x-y position in the stack is shown. Fig. 1 *e* shows a y-z maximum projection of the same cells. Fig. 1 *f* shows that the TGN is next to the ERC and may encircle it, and Fig. 1 *e* shows that the TGN is at a different vertical position in the cell. Even though parts of the TGN may look as if they occupy the same area as the ERC when viewed in an x-y projection (*arrow* in Fig. 1 *f*), the y-z projection reveals that this is not so (*arrow* in Fig. 1 *e*). Thus, although both the TGN and the ERC are next to the nucleus, these figures demonstrate that the TGN and the ERC are in different intracellular locations which can be resolved by confocal microscopy.

Kinetics of TacTGN38 Appearance on the Cell Surface

The above analysis shows that TacTGN38 is correctly targeted to the TGN in transfected CHO cells. We used this system to analyze the kinetics of trafficking from the surface to the TGN and back to the surface. To determine how long it takes TacTGN38 to cycle from inside the cell to the plasma membrane, cells were incubated with Cy3 anti-Tac Fab for different times. The entire 3-D stack of the cell was imaged by confocal microscopy, and the Cy3 fluorescence power per cell was measured. A corresponding differential interference contrast microscopy (DIC)

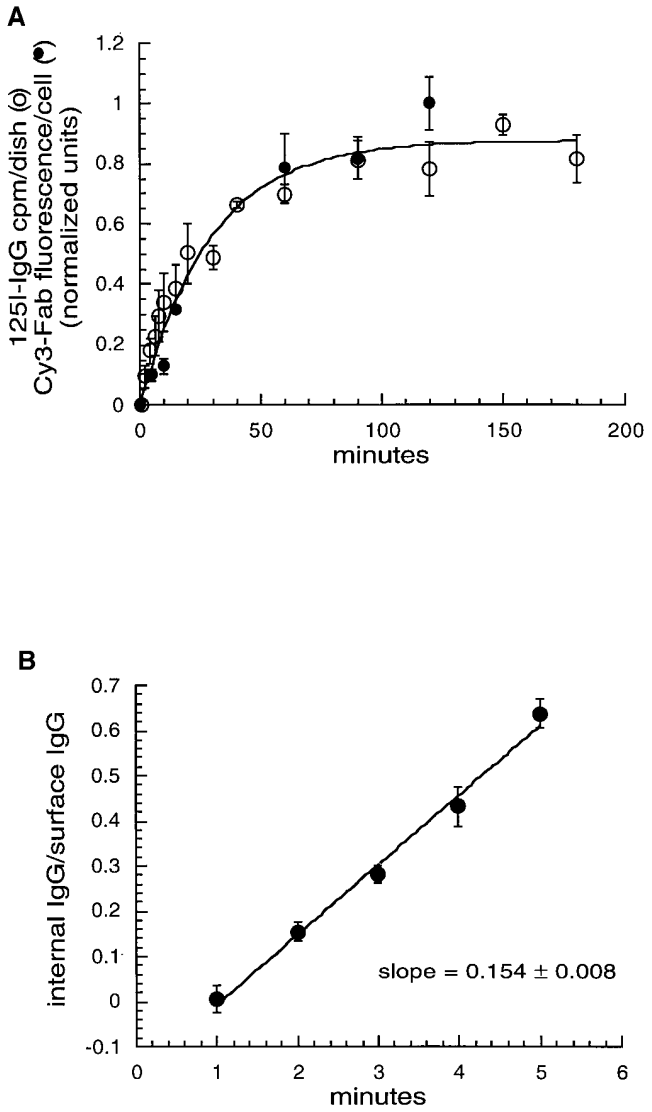

Figure 2. Time course for TacTGN38 delivery to the cell surface and internalization from the cell surface. (*A*) Cells were incubated either with [^{125}I]anti-Tac IgG (○) or Cy3 anti-Tac Fab (●) for the times shown. The cells were fixed, and the amount of endocytosed anti-Tac antibody in the cell was assessed either by radioactivity counting or quantifying the fluorescence intensity in 3-D stacks of images taken of the whole cell by confocal microscopy. Background values were subtracted (0-min value), and the data were normalized so that the fluorescence and ^{125}I curves could be superimposed. It takes over 1 h for endocytosed anti-Tac to reach steady state, and fluorescence quantification gives the same kinetic data as ^{125}I measurements. (*B*) Cells were incubated with [^{125}I]anti-Tac IgG for brief periods of time, and the surface-bound and internalized counts were determined. The ratio of internalized-to-surface counts is plotted, and it increases linearly over time with a slope of 0.154 min^{-1}. Error bars represent SEM.

image was taken in order to count the number of cells. For each 3-D stack of images, the background was subtracted from each individual slice, and the integrated intensity in all the slices was summed. In such an accumulation experiment, the rate constant controlling the approach to steady-state is the rate for the probe to go from inside the cell to the plasma membrane. We have previously discussed this fact in detail for the case of approach to steady-state of internalized Tf in the whole cell (9). Fig. 2 *a* (*closed circles*) shows the accumulation of anti-Tac Fab in cells over time. The increase at early times is due to Cy3-Fab binding to unoccupied TacTGN38 molecules as they appear on the cell surface, and the flattening of the curve at later times shows that the amount of Cy3-Fab per cell comes to a steady state.

The appearance of TacTGN38 on the cell surface was also measured using [^{125}I]anti-Tac IgG. Cells were incubated with [^{125}I]anti-Tac IgG for increasing lengths of time at 37°C, and the cell-associated radioactivity was measured. As shown in Fig. 2 *a* (*open circles*), the rate of accumulation of [^{125}I]anti-Tac IgG was similar to the accumulation of the Cy3 anti-Tac Fab. These studies confirm that fluorescence measurements can be used to obtain kinetic data on the accumulation of anti-Tac in cells. The data show that the entire cycling pool of TacTGN38 becomes labeled within about 2 h. We could not determine from these experiments whether the appearance of TacTGN38 on the cell surface represented a single first order process or multiple processes. As indicated in later sections, there is evidence for multiple processes, so we do not report kinetic parameters for the overall appearance on the surface.

The size of the total pool of cycling TacTGN38 is determined from the asymptote of the accumulation curve, and we estimate that there are 1.5×10^6 copies of TacTGN38 per cell. When cells were incubated with [^{125}I]anti-Tac IgG at 0°C, we found ~160,000 TacTGN38 molecules per cell on the plasma membrane (see Table II). The number of TacTGN38 molecules on the cell surface is comparable to the levels of Tf receptor at the plasma membrane of TRVb1 cells (30). We also isolated cells expressing 10-fold less TacTGN38 than the cells used in this study, and found similar intracellular distributions as in the cells used in this study.

Internalization of TacTGN38 into Early Endosomes

To measure the rate of internalization from the cell surface, [^{125}I]anti-Tac IgG was applied to cells for a brief period, after which the surface-bound and internalized counts were determined by acid stripping for each time point as described in Materials and Methods. The ratio of internalized-to-surface counts increased linearly over time with a slope (k_i) of 0.15 min^{-1}, as shown in Fig. 2 *b*. This internalization rate constant is similar to that of Tf receptors in TRVb1 cells (31), indicating that TacTGN38 is rapidly cleared from the cell surface. This is consistent with previous studies which have shown that the YQRL sequence in the cytoplasmic domain of TGN38 is an efficient coated pit internalization motif (3, 15, 49).

To follow TacTGN38's initial internalization steps, we compared its trafficking with Tf, which trafficks through sorting endosomes and the ERC before returning to the plasma membrane. Cells were coincubated with 1 μg/ml Alexa488 anti-Tac IgG and 3 μg/ml Cy3-Tf for 10 min. The cells were fixed, and 3-D images through the entire thickness of the cells were obtained by confocal microscopy. Tf (Fig. 3 *a*) and anti-Tac IgG (Fig. 3 *b*) are colocalized in small punctate structures that are presumably sort-

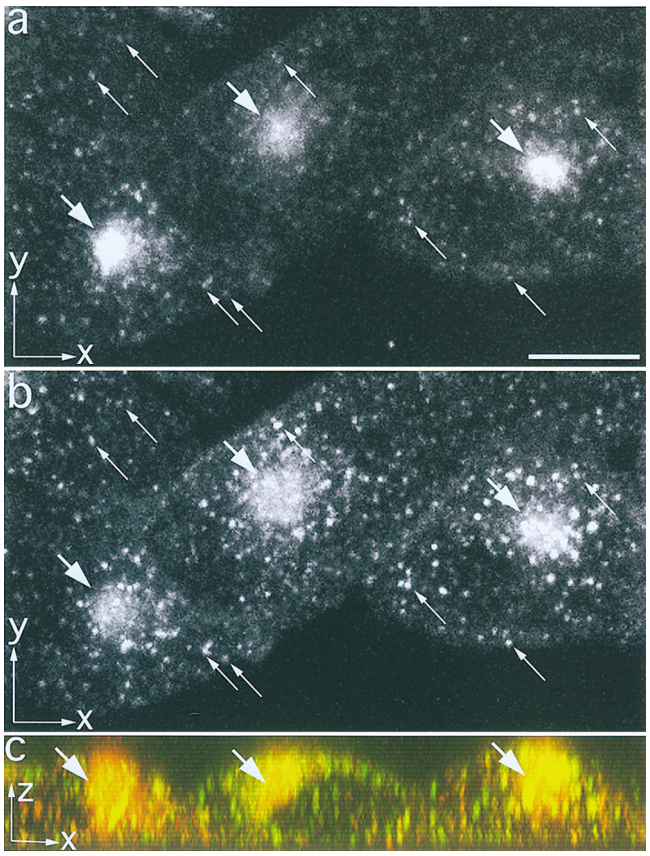

Figure 3. TacTGN38 overlaps with Tf in the endocytic recycling compartment. Cells were coincubated for 10 min with Cy3-Tf (*a*) and Alexa488-anti-Tac IgG (*b*). Images were obtained by confocal microscopy, and maximum x-y projections are shown in *a* and *b*. The long slender arrows show colocalization in punctate endosomes, and the short thick arrows show colocalization in the perinuclear ERC. An x-z maximum projection of the same cells is shown in *c*. Cy3-Tf is in red, Alexa488-IgG is in green, and their colocalization in the ERC is seen ranging from orange to yellow (*thick arrows*). Bar, 10 μm.

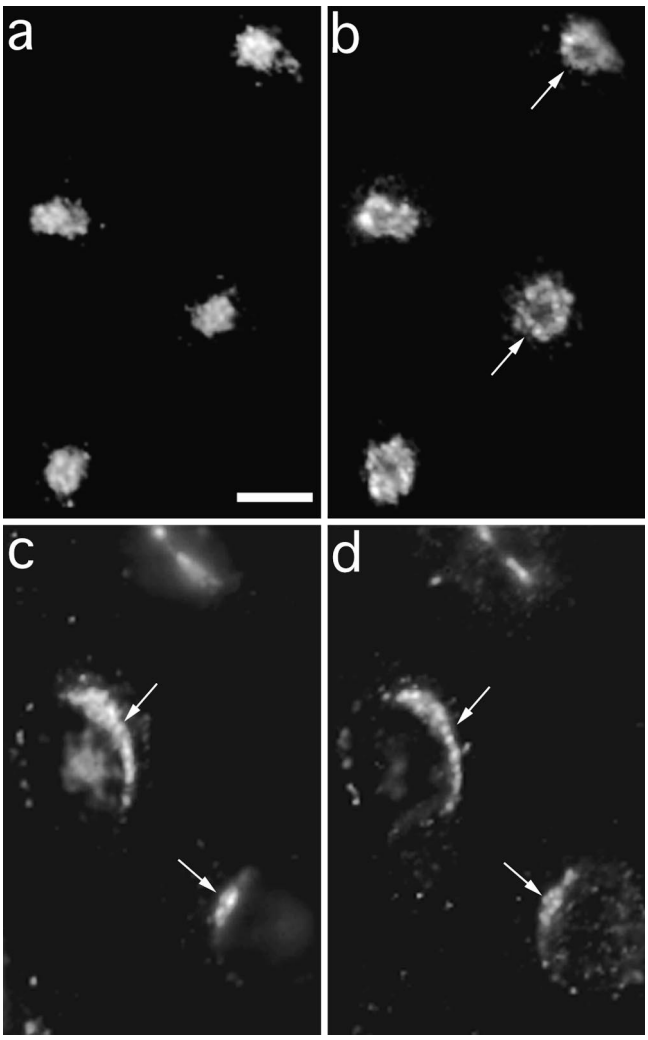

Figure 4. Internalized anti-Tac colocalizes with furin after a 60-min chase. Cells were incubated with 4 mg/ml anti-Tac monoclonal antibodies conjugated to Alexa 488 fluorescent dye (*a* and *c*) for 10 min. Cells were fixed immediately (*a* and *b*) or chased in medium for 60 min (*c* and *d*). After fixation, cells were permeabilized and stained with polyclonal antibodies against furin (*b* and *d*) followed by rhodamine-conjugated goat anti–rabbit secondary antibodies. In the absence of a chase, anti-Tac was detected in a distribution that resembles the endocytic recycling compartment, and is surrounded by the TGN (*arrows*) as labeled by anti-furin antibodies. With a 60-min chase, anti-Tac predominantly colocalized with furin (*arrows*). Bar, 5 μm.

ing endosomes (*thin arrows*) as well as in the juxtanuclear ERC (*thick arrows*). To ensure that the large structures (*thick arrows*) in Fig. 3, *a* and *b* were not at different elevations in the cell and were truly colocalized, we also viewed the cells as a maximum vertical (x-z) projection (Fig. 3 *c*). The Cy3-Tf (*red*) and the Alexa488 anti-Tac IgG (*green*) are colocalized in the vertical dimension, as seen by the orange-yellow staining (*thick arrows*).

When cells internalized Alexa488 anti-Tac IgG for 10 min and were then fixed, the anti-Tac IgG is in a structure resembling the ERC (Fig. 4 *a*) surrounded by the TGN (Fig. 4 *b; arrows*). The rapid appearance of internalized TacTGN38 in the ERC is similar to the rate at which Tf begins to appear in this compartment (6, 9, 29). After short incubations, endocytosed TacTGN38 colocalized with Tf in all the clonal lines we examined. In addition, anti-Tac IgG and Fab that were cointernalized for 10 min colocalized into small punctate endosomes and a juxtanuclear compartment resembling the ERC (not shown). This colocalization demonstrates that the appearance of anti-Tac IgG in the ERC is not a consequence of using bivalent antibody. A different endocytosed monoclonal anti-Tac antibody, prepared from the 7G7b6 hybridoma cell line, was also delivered to the ERC after short incubations, and to the TGN after a prolonged chase (data not shown), demonstrating that the trafficking to the ERC is not due to the particular anti-Tac antibody being used.

TacTGN38 Fluorescence in the ERC Can Be Ablated by HRP-Tf

Since the TGN is in close proximity to the ERC, it is important to verify that endocytosed anti-Tac IgG colocal-

izes with Tf in the ERC after short incubation times. We used an HRP fluorescence ablation technique (29a) that extinguishes the fluorescence from any fluorescent probe that is in the same compartment as HRP. We coincubated cells with fluorescent IgG and HRP-Tf, and then treated the cells with hydrogen peroxide and DAB. HRP-Tf binds to the TR and trafficks to the ERC. The HRP-catalyzed DAB reaction product will ablate the fluorescence from fluorophores in the same compartment as the HRP-Tf (29a). We first did a positive control to check that the fluorescence in the ERC was being quenched. We incubated cells with 1 μg/ml Cy3-Tf for 10 min, chased for 10 min with 50 μg/ml HRP-Tf, and fixed and treated the cells with hydrogen peroxide and DAB. The DAB reaction quenched most of the Cy3-Tf in the ERC (Fig. 5 *b*). To ensure the DAB reaction was not nonspecifically quenching cell fluorescence, we carried out the same protocol but also included excess unlabeled Tf (5 mg/ml) in the chase media along with the HRP-Tf. The excess unlabeled Tf prevents significant HRP-Tf binding to the TR and uptake into cells, and thus the cells are still fluorescent after the DAB reaction (Fig. 5 *a*). These controls demonstrate that we can quench Cy3 fluorescence in the same compartment as HRP-Tf, and that this quenching is specific. We next incubated cells with 1 μg/ml Cy3 anti-Tac IgG for 10 min, and then chased for 10 min with 50 μg/ml HRP-Tf with or without excess unlabeled Tf. In cells that had internalized Cy3-IgG and were chased with excess unlabeled Tf, the Cy3-IgG was in a large perinuclear area consistent with labeling of both the ERC and the TGN (Fig. 5 *c*). When there was no unlabeled Tf present in the chase, the HRP-Tf reached the ERC; the DAB reaction quenched the center of the perinuclear staining (*arrows*), but a ring of Cy3-IgG staining remained (Fig. 5 *d*). The fluorescence loss in the center of the structure shows that after 20 min, some of the Cy3-IgG was in the ERC. The fluorescence that remained unquenched was in a ring pattern characteristic of the TGN. In cells that had been incubated with Cy3 anti-Tac IgG for 50 min and then with HRP-Tf for an additional 10 min (total time is 60 min), and then treated with DAB and hydrogen peroxide, a similar pattern as seen in Fig. 5 *d* was obtained, except that the remaining ring stain was much brighter (data not shown). This result is consistent with increased accumulation of Cy3-IgG in the TGN where it would not be quenched by the HRP reaction.

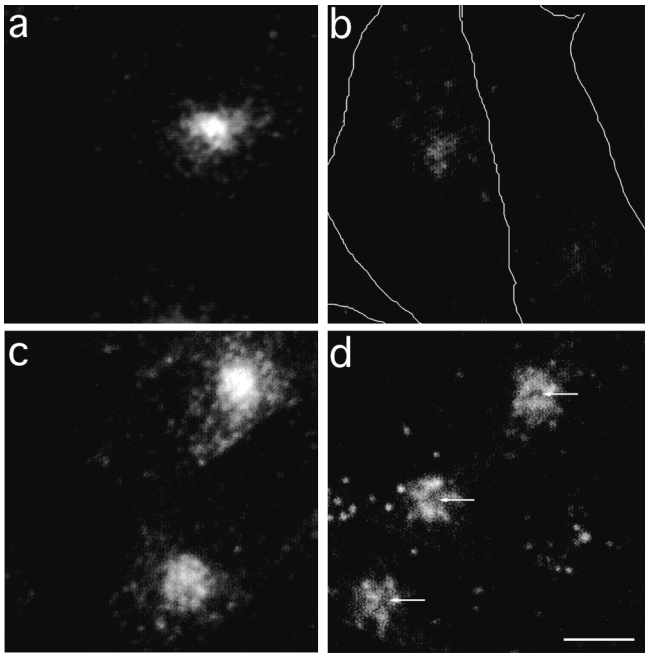

Figure 5. TacTGN38 overlaps with Tf in the ERC, as shown by HRP ablation. Cells were incubated with 5 μg/ml Cy3-Tf for 30 min, and were then chased for 10 min with 50 μg/ml HRP-Tf with (*a*) or without (*b*) excess (5 mg/ml) unlabeled Tf. The cells were then treated with hydrogen peroxide and DAB. The reaction products of the DAB reaction quenched fluorescence from molecules contained in the same compartment as the HRP-Tf (*b*), and the unlabeled Tf competed with HRP-Tf for binding to the TR and prevented quenching of the Cy3-Tf fluorescence (*a*). The cell boundaries, determined by DIC microscopy, are shown in *b*. Cells were also incubated with 1 μg/ml Cy3 anti-Tac IgG for 10 min, and were then chased for 10 min with 50 μg/ml HRP-Tf with (*c*) or without (*d*) 5 mg/ml unlabeled Tf. The DAB reaction with the HRP-Tf in the ERC quenched the Cy3-IgG fluorescence in this compartment (*d*), leaving a dark area (*arrows*) surrounded by the ring staining of the Cy3-IgG characteristic of the TGN. The fluorescence images show a summation projection of slices in a 3-D stack obtained by confocal microscopy. Bar, 10 μm.

Approximately 80% of Tac-TGN Is Delivered from the ERC to the Plasma Membrane with a Half-time of 9 Min

Since internalized TacTGN38 enters the ERC, we examined whether a fraction of it is returned to the cell surface. After long incubations, internalized anti-Tac antibodies are mainly in the TGN (Fig. 1), but after brief incubations most of the anti-Tac is still in early endosomes (i.e., sorting endosomes and ERC; Fig. 3). To measure TacTGN38's recycling rate to the plasma membrane after endocytosis, TRVb1 cells were incubated with fluorescein-labeled anti-Tac IgG for 5 min, followed by incubation in the presence of antifluorescein antibodies from 5 to 40 min. We verified that the antifluorescein antibodies quench fluorescein-conjugated anti-Tac antibody (F-anti-Tac) fluorescence by ~90% upon binding as reported previously for other fluorescein labeled proteins (41, 42). At the concentration used in our studies, essentially no antifluorescein antibody reached either the ERC or the TGN in the absence of F-anti-Tac, as observed by labeling with secondary antibodies (data not shown; see references 41 and 42). In contrast, antifluorescein was readily detected in cells that had been loaded previously with F-anti-Tac. Since fluorescence quenching requires a stoichiometric interaction of antifluorescein with F-anti-Tac, a decrease in fluorescence is due mainly to the fluorescein-conjugated IgG (F-IgG) that reaches the plasma membrane being quenched by the antifluorescein antibodies in the extracellular media.

Initially, the anti-Tac IgG is in structures that resemble the ERC (see Fig. 3). The cells showed a loss of fluorescence over time, and the residual intracellular fluorescence after a 40-min chase was in a crescent-shaped structure characteristic of the TGN (not shown). The loss of

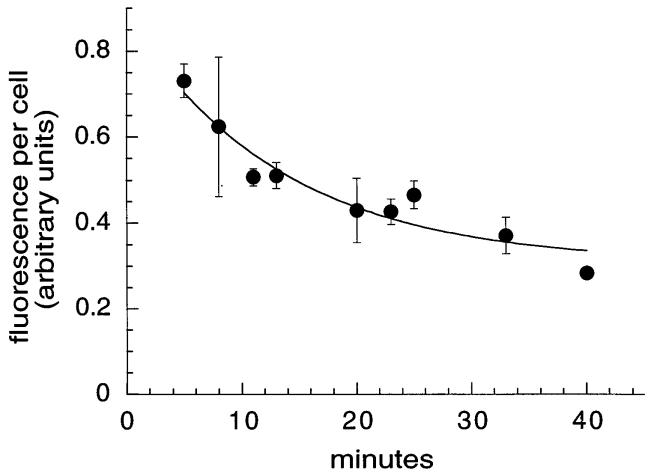

Figure 6. TacTGN38 trafficks from the recycling compartment to the plasma membrane with a half-time of 9.5 min. Cells were pulsed for 5 min with 1 μg/ml F-anti-Tac IgG followed by chases with medium containing 10 μg/ml anti-fluorescein antibodies. The recycled TacTGN38 was quenched as it returned to the cell surface. Fluorescence images were obtained by wide-field microscopy and fluorescence power per cell was measured. The fluorescence power was fit to a monoexponential decay that gave a half-time of TacTGN38 recycling to the plasma membrane of 9.5 min. Error bars represent SEM.

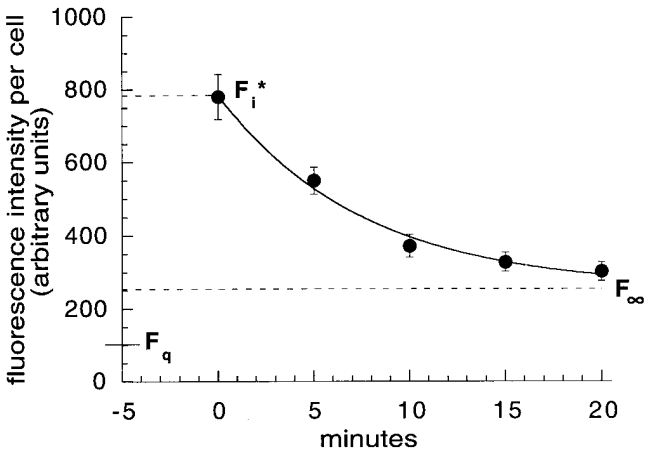

Figure 7. 18% of TacTGN38 is delivered to TGN with each round of endocytosis. Cells were labeled with 1 μg/ml F-anti-Tac IgG on ice, and were then warmed for 5 min, washed, and chased with 10 μg/ml anti-fluorescein antibodies. Fluorescence images were obtained by wide-field microscopy, quantified, and fit to a monoexponential decay. Data from a representative experiment are shown. The asymptote gave the residual fluorescence F_∞, and a cell that was fixed and imaged without warming gave the initial cell-associated fluorescence, F_i*. F_q is the residual fluorescence after quenching surface bound anti-Tac. Error bars represent SEM.

fluorescence was quantified by determining the cell-associated fluorescence power per cell as described in Materials and Methods. Chase times were kept relatively brief to analyze only the fluorescent probe that was transported directly from the early endosomes to the plasma membrane. Fig. 6 shows the time course of the loss of fluorescence. If we assume that only a fraction of the internalized anti-Tac will recycle rapidly, then the loss of fluorescence corresponding to that fraction could be well fit by a single exponential decay with a nonzero asymptote, giving a half-time of 9.5 min as shown by the solid line in Fig. 6. This rate of return of anti-Tac to the cell surface is similar to the rate of return of Tf receptors from the ERC to the cell surface (29, 31, 38).

These observations imply that a fraction of TacTGN38 is diverted to the TGN with each cycle of endocytosis and recycling. To measure the recycling from a single round of endocytosis directly, anti-Tac IgG was bound to cells at 0°C, and the cells were then warmed to 37°C for 5 min to allow internalization of the antibody. Cells then were incubated further for 5, 10, 15, and 20 min in the presence of antifluorescein antibody, followed by fixation. This time course should allow most of the recycling pool of TacTGN38 to be externalized from the recycling endosome, without a significant amount being delivered to the TGN and then being externalized from there. Fluorescence intensities per cell were determined, and data from a representative experiment are shown in Fig. 7. It can be seen that most of the internalized F-anti-Tac becomes exposed to the extracellular antifluorescein antibody with a half-time of ~10 min, but there is a residual fluorescence that remains unquenched. This residual fluorescence is significantly above the fluorescence, F_q, that would be found if all the cell-associated F-anti-Tac were exposed to antifluorescein antibody.

We modeled the recycling (i.e., exposure to the extracellular antifluorescein antibody) as a first-order rate process with a fraction of nonrecycling F-anti-Tac. In four independent experiments, the nonrecycling pool was found to be 18.1 ± 3.4% of the F-anti-Tac that was internalized in the initial pulse (Table I). We presume that this 18% of internalized anti-Tac represents the fraction that is delivered to the TGN on each round of endocytosis. The half-times for recycling derived from these experiments varied from 8.8 to 11.9 min, which is consistent with the recycling rate reported in Fig. 6.

TacTGN38 Does Not Accumulate in Late Endosomes before Entry into the TGN

To determine whether TacTGN38 accumulates in late endosomes en route to the TGN, we incubated cells with fluorescein-dextran (F-dex) and with either Cy3-anti-Tac IgG or rhodamine-dextran (R-dex) for 10 min, chased for 20 min, then obtained single optical sections by confocal microscopy at a focal position that showed intense labeling of the F-dex. Both dextrans and anti-Tac IgG are initially in sorting endosomes (Fig. 3). Since the half-time for a sorting endosome to mature into a late endosome is 6–8 min (5, 41, 42), after a 20-min chase ~80–90% of the dextran-labeled endosomes would have matured into late endosomes.

If the late endosome is a major pathway for delivery of internalized TacTGN38 to the TGN, there should be significant colocalization between fluorescein dextran and Cy3-IgG after 20 min. Fig. 8 shows single confocal slices at

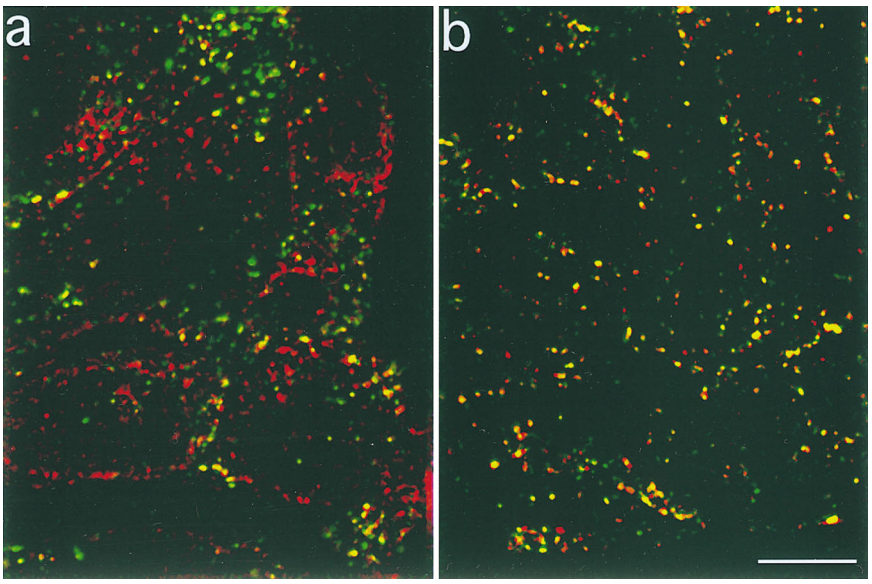

Figure 8. Little TacTGN38 is seen in late endosomes. Cells were coincubated with fluorescein dextran, and either with Cy3-IgG (*a*) or rhodamine dextran (*b*) for 10 min and then chased for 20 min. Images were obtained by confocal microscopy, and single slices are shown. Fluorescein dextran is shown in green, Cy3-IgG and rhodamine dextran are shown in red, and colocalized areas range from orange to yellow. After a 20-min chase, the fluorescein dextran is much less colocalized with the Cy3-IgG (*a*) than with the rhodamine dextran (*b*). Bar, 10 μm.

a focal plane that contains several late endosomes. Relatively little colocalization is seen at this time (Fig. 8 *a*), and structures labeled with only one probe were readily detected (*red* and *green* labeling in Fig. 8 *a*). Some fluorescein–dextran-containing spots also contained Cy3-IgG, but we are unable to determine if these are late endosomes or sorting endosomes that have not as yet matured. As a positive control we cointernalized R-dex and F-dex for 10 min, followed by a 20-min chase. We see good colocalization of R-dex and F-dex because the majority of spots range from orange to yellow in Fig. 8 *b*. Although R-dex and F-dex traffic similarly and are colocalized in the same compartments, the amount of both dextrans in an individual endosome may not be equal. These data suggest that late endosomes are not major intermediates in the delivery of TacTGN38 from the recycling pathway to the TGN, or that TacTGN38 passes through late endosomes too rapidly to be detected by our methods. Further experiments are necessary to distinguish between these possibilities.

Kinetics of Trafficking TacTGN38 into and out of the TGN

To determine how rapidly TacTGN38 internalized from the cell surface begins to appear in the TGN, we incubated cells at 37°C for 10 min with Cy3-anti-Tac Fab, and then further incubated the cells in media lacking Cy3-Fab. The cells were then fixed and labeled with C_6-NBD–ceramide to identify the TGN. Single confocal slices were obtained at a position corresponding to the NBD-labeled TGN (Fig. 9). Fig. 9 *b* shows the Cy3-Fab distribution after a 10-min incubation with no chase. Fig. 9 *a* shows the corresponding C_6-NBD-ceramide image. Some Cy3-Fab is seen colocalized with the C_6-NBD-ceramide–labeled TGN (see *arrows*), although the amount of anti-Tac in the TGN is low. After a 10-min pulse and a 10-min chase there is much more Cy3-Fab that overlaps the C_6-NBD-ceramide labeling (Fig. 9, *c* and *d*). These data indicate that TacTGN38

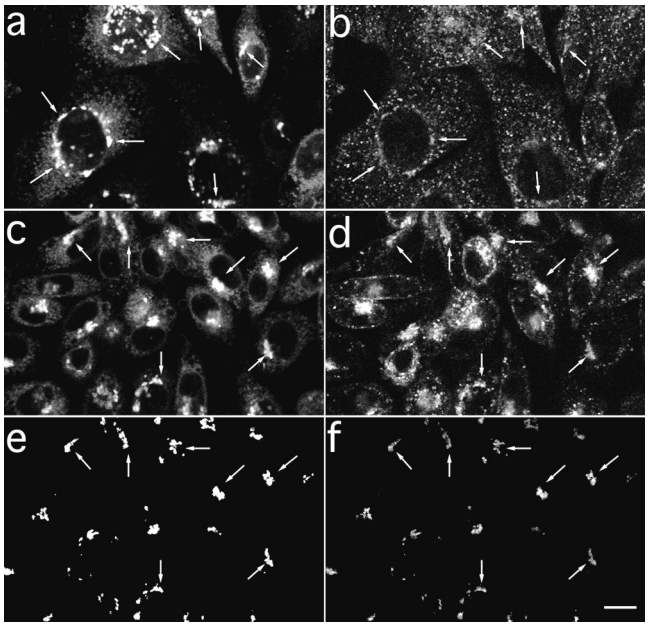

Figure 9. TacTGN38 reaches the TGN soon after internalization. Cells were pulse-labeled with Cy3-Fab for 10 min before being chased for either 0 or 10 min. The cells were then fixed, and the TGN was stained with C_6-NBD-ceramide. Single-slice images were obtained by confocal microscopy. (*a* and *b*, 0-min chase) Some Cy3-Fab (*b, arrows*) is already seen in the NBD-stained TGN (*a*, *arrows*). (*c* and *d*, 10-min chase) A larger amount of Cy3-Fab (*d*, *arrows*) is in the TGN (*c*, *arrows*). (*e* and *f*) Image-processing steps used to determine the amount of Cy3-Fab in C_6NBD-ceramide-labeled TGN. Background subtraction and thresholding of *c* is used to generate the mask of the C_6-NBD-ceramide–labeled TGN as shown in *e*. After background-subtracting *d*, the mask in *e* is applied to *d* to select those Cy3-Fab pixels that overlap with the C_6-NBD-ceramide labeling, and the result is shown in *f*. Arrows in *c–f* indicate the selected overlapping areas. The intensity of the selected Cy3 pixels are summed and then normalized by the number of pixels in the mask to give the Cy3 fluorescence per NBD-labeled pixel. Bar, 10 μm.

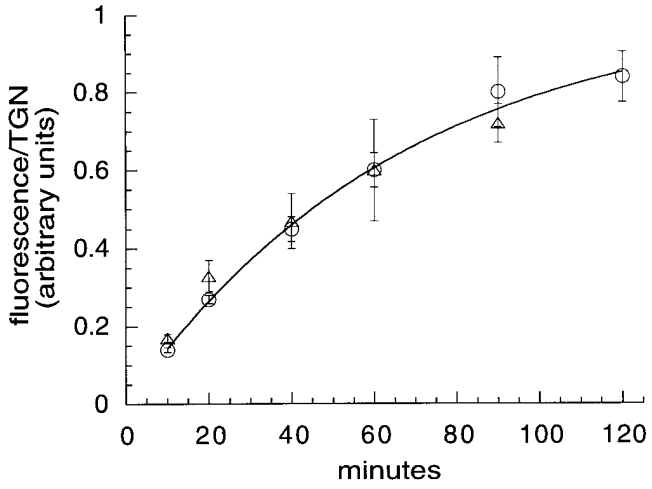

Figure 10. Accumulation of TacTGN38 in the TGN. Cells were incubated with F-anti-Tac IgG for the times shown, fixed, and labeled with Cy3-anti-Tac IgG. Confocal microscopy was used to obtain the entire 3-D distribution through the cell, and these images were quantified to determine the amount of F-IgG per TGN volume element (○). The data were fit to a kinetic approach to steady state with a half-time of 46 min. Cells were also incubated with Cy3-anti-Tac Fab for different times, and then the TGN was stained with C_6NBD-ceramide. Single slice images were obtained by confocal microscopy. Quantification of the amount of Cy3-Fab fluorescence per TGN area (see Fig. 9, *c–f*) also gave a half-time of 46 min (△). Error bars represent SEM.

begins to enter the TGN within minutes after it is internalized.

To measure the rate of accumulation of TacTGN38 in the TGN, cells were allowed to internalize Cy3-Fab for different times, fixed, and labeled by C_6-NBD-ceramide. Quantifying the accumulation will give the kinetics of approach to steady-state labeling of the TGN by internalized TacTGN38. Single confocal slices were obtained at a position corresponding to the NBD-labeled TGN, and the amount of Cy3 fluorescence per NBD-labeled pixel was quantified as described in Materials and Methods. Our image-processing steps are demonstrated in Fig. 9 (*c–f*). In short, background subtraction and intensity thresholding of the C_6-NBD-ceramide–labeled image (Fig. 9 *c*) gives a mask image (Fig. 9 *e*) that delineates the NBD-labeled areas from the background cellular fluorescence. This mask image (Fig. 9 *e*) is applied to the Cy3-labeled image (Fig. 9 *d*) that has first been corrected for background to select those Cy3 pixels that are colocalized with the C_6-NBD-ceramide, and the result is shown in Fig. 9 *f*. Arrows in Fig. 9, *c–f* indicate the colocalized selected structures. The intensity of the selected Cy3 pixels in Fig. 9 *f* are summed and then divided by the number of pixels in the NBD mask, giving the Cy3 intensity per TGN area (i.e., NBD pixel). These image-processing steps were applied to cells that were incubated with Cy3-Fab for different times and then labeled with C_6-NBD-ceramide after fixation. The data are plotted in Fig. 10 (*triangles*). The approach to steady-state labeling could be described by a single first-order process with a $t_{1/2}$ of 46 min (Table I).

The approach to steady-state labeling in the TGN was also determined in cells that had been incubated with fluorescein-conjugated anti-Tac IgG for different times, fixed, permeabilized, and labeled with Cy3 anti-Tac IgG. Confocal microscopy was used to image the entire 3-D distribution of both fluorescent probes through the cell. Since at steady-state TacTGN38 is mostly concentrated in the TGN, we can use its presence as a marker for the TGN (see Cy3 anti-Tac IgG labeling in Fig. 1, *e* and *f*). The amount of fluorescein anti-Tac that overlaps with the Cy3-labeled TGN at different times can be used to measure the accumulation of internalized TacTGN38 into the TGN.

We carried out a quantitative analysis to determine the amount of endocytosed TacTGN38 reaching the TGN at different times in a manner similar to that shown in Fig. 9, *e* and *f* (see Materials and Methods). We used the Cy3-IgG image as a mask, and determined the amount of fluorescein fluorescence in it. This was done for every slice in the 3-D stack of the cell. The amount of fluorescein was divided by the total number of the voxels (3-D pixels or volume elements) covered by the Cy3-labeled TGN structure to give the amount of fluorescein per Cy3-labeled TGN volume element. These data are shown in Fig. 10 (*circles*). The approach to steady-state labeling could also be described by a single first-order process with a $t_{1/2}$ of 46 min (Table I), and the time course is indistinguishable from the

Table I. Summary of Kinetic Parameters

Kinetic step	Measurement technique	No. of experiments (no. of fields per time point)	Fig.	Rate constant	Half-time
				min^{-1}	*min*
Internalization	[^{125}I] IgG internal/surface ratio over short times	4 (3)	2 *b*	0.154 ± 0.008	4.5
	F-IgG accumulation in TGN obtained by 3-D confocal stacks	1 (5)	10	0.015 ± 0.002	46
TGN to plasma membrane rate (k_T)	Cy3-Fab accumulation in C_6-NBD-ceramide labeled TGN	2 (5)	10	0.015 ± 0.005	46
	Quenching of F-IgG exiting TGN	3 (10)	11	0.015 ± 0.002	46
Recycling compartment-to-plasma membrane rate* (k_E)	Quenching of F-IgG exiting compartment recycling	4 (10)	6	0.073 ± 0.032	9.5

*% of TacTGN38 delivered to TGN (determined by quenching of F-IgG exiting recycling compartment) is: 18.1 ± 3.4%; (4 experiments, 10 fields per time point; Fig. 7).

results obtained from quantifying the Cy3-Fab entry into C_6-NBD-ceramide labeled TGN in single confocal slices.

Since the total pool of TacTGN38 is approximately at steady state, the rate of filling the TGN should be balanced by the rate at which TacTGN38 leaves the TGN, and both processes should have a $t_{1/2}$ of 46 min. We directly measured the rate at which TacTGN38 goes from the TGN to the cell surface by using the quenching of fluorescein fluorescence by antifluorescein antibodies. Fluorescein-labeled anti-Tac IgG was accumulated within the TGN by pulse labeling the cells for 10 min, and then washing and chasing the cells with medium without F-IgG for another 50 min. The F-IgG intracellular distribution was in a perinuclear structure consistent with localization mainly in the TGN (see Fig. 1). After the chase, antifluorescein antibodies were added to the medium, and the loss of fluorescein fluorescence over time was measured. This decrease in fluorescence is due to the F-IgG that reaches the plasma membrane being quenched by the antifluorescein antibodies in the extracellular media. Fluorescence microscopy confirmed the diminution of fluorescence in the TGN over time in the presence, but not in the absence of antifluorescein antibodies. Fig. 11 *a* shows images of cells obtained by wide-field fluorescence microscopy after 10 min of antifluorescein antibody application, and Fig. 11 *b* shows cells that have been chased with antifluorescein antibody for 180 min. The fluorescence intensity is greatly reduced after the 180-min chase. The fluorescence power per cell was determined as described in Materials and Methods. As shown in Fig. 11 *c*, the loss of fluorescence could be fit to a monoexponential decay ($t_{1/2}$ = 46 min; Table I). By comparing the asymptote of Fig. 11 *c* with that of Fig. 6, we can estimate that ~18% of endocytosed F-anti-Tac is delivered to the TGN without undergoing endocytic recycling, which agrees with the value measured directly (Fig. 7). The antifluorescein antibody did not alter the trafficking of TacTGN38 since after binding to anti-Tac the antifluorescein antibody was delivered efficiently to the TGN (not shown).

Thus, by three independent methods measuring the traffic from the cell surface to the TGN or from the TGN to the cell surface, we find that TacTGN38 trafficks between the TGN and the cell surface with a half-time of ~46 min (Table I).

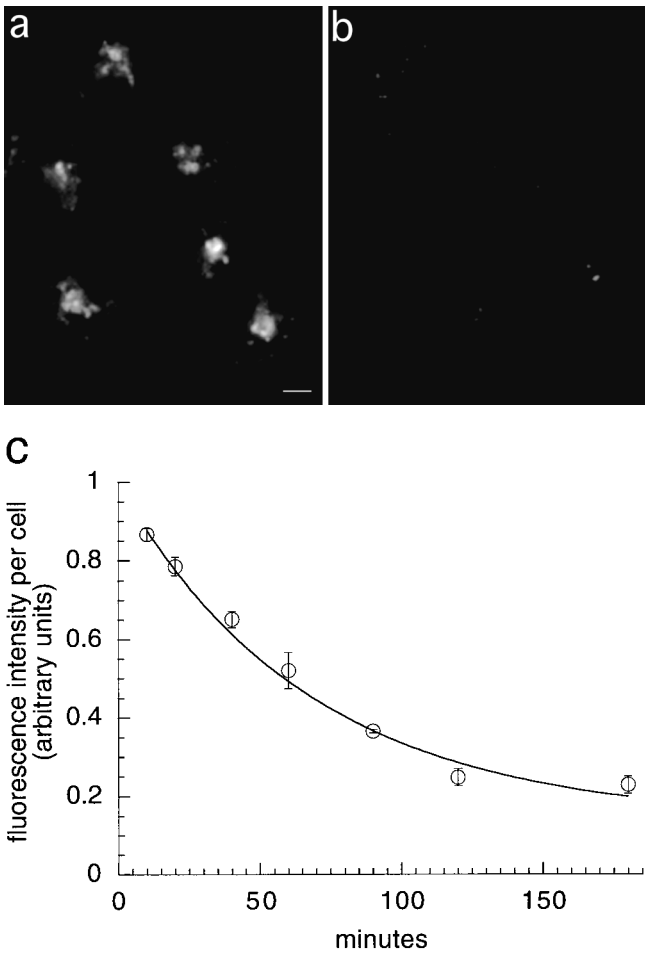

Figure 11. TacTGN38 goes from the TGN to the plasma membrane with a half-time of 46 min. Cells were pulsed with 1 μg/ml F-anti-Tac IgG for 10 min, and were then chased for 50 min. The cells were then incubated with 10 μg/ml anti-fluorescein antibodies that quench the fluorescence of F-IgG that returns to the cell surface. Images obtained by wide-field microscopy show that from 10 (*a*) to 180 min (*b*) in the presence of anti-fluorescein antibody, fluorescence quenching has occurred. The fluorescence intensity was quantified to determine the loss of fluorescence in the cell over time (*c*). When fit to a monoexponential decay, the efflux kinetics show a half-time of 46 min for TacTGN38 to go from the TGN to the plasma membrane. Bar, 10μm; error bars represent SD.

Discussion

Although the major cellular localization of TGN38 is the TGN, a small percentage of TGN38 is found on the cell surface (1). The TGN38 on the surface is internalized and delivered to the TGN (23, 40). However, it has not been known which postendocytic pathways TGN38 follows from the cell surface to the TGN. Most membrane constituents recycle back to the plasma membrane either by a rapid recycling pathway ($t_{1/2} \sim 2$ min; 2, 38) or via the ERC ($t_{1/2} \sim 10$ min). Some membrane proteins are recycled slowly, and are either retained intracellularly (e.g., GLUT4; 16) or are delivered to late endosomes (e.g., M6PR; 22). Efficient recycling of membrane constituents is favored by the physical properties of the early endosomes (34), and specific peptide sequences or motifs are associated with intracellular retention or delivery to late endosomes (14, 19, 20, 35). TGN38 has been shown to carry such information in its cytoplasmic and transmembrane domains (3, 15, 37, 49). A cytoplasmic sequence, SDYQRL, is sufficient to promote rapid internalization by the receptor-mediated endocytosis pathway, but this sequence is not sufficient to direct delivery to the TGN (18). TacTGN38, which has the entire transmembrane and cytoplasmic sequence of TGN38, has been shown previously to enter the TGN and to have a steady-state distribution very similar to TGN38 (15, 39), and our studies confirm the predominant TGN distribution of TacTGN38.

A major goal of this study was to analyze the kinetics of trafficking from the surface to the TGN. We found that TacTGN38 entered the ERC rapidly after internalization. In fact, after short incubations with anti-Tac antibodies,

the ERC was the major compartment that became labeled (Fig. 3). TacTGN38 was internalized at a similar rate as Tf (Fig. 2 *b* and Table I), and could also be seen in small punctate compartments that contained Tf, and that have been shown in previous studies to be sorting endosomes (6, 9, 29). These data indicated that for the first few minutes after internalization, TacTGN38 followed the same itinerary as internalized Tf. This colocalization was further demonstrated by coincubating cells with Cy3 anti-Tac IgG and HRP-Tf. When the HRP-catalyzed reaction with DAB was performed, the Cy3 fluorescence in the ERC was extinguished, showing that the Cy3-IgG was in the same compartment as the HRP-Tf (Fig. 5). We could not detect significant accumulation of anti-TacTGN38 in late endosomes that were labeled with internalized dextran (Fig. 8). Thus, most internalized TacTGN38 passes through the ERC.

What is the fate of TacTGN38 after it passes through the ERC? Most of the internalized TacTGN38 returns to the cell surface, but ~18% is retained inside the cell. This was shown by loading fluorescein anti-Tac into the ERC by short incubations followed by a chase with antifluorescein antibody in the chase medium. Under these conditions, fluorescein-labeled antibodies are quenched when they return to the surface. In each round of internalization, ~82% of the anti-Tac was returned to the surface with a $t_{1/2}$ of 9.5 min, which is within experimental error of the rate of return of recycling Tf receptors (29, 31, 38). This result indicated that a TGN38 molecule on the cell surface would recycle several times, on average, before being delivered to the TGN.

The fluorescence that remained in the cells after chasing in the presence of antifluorescein antibodies showed a distribution characteristic of the TGN. Since this fluorescence was not quenched by the antifluorescein antibodies, it must have moved to the TGN by an intracellular route. However, it remains unclear precisely how TacTGN38 moves from the ERC to the TGN. We can detect endocytosed TacTGN38 in the TGN as early as 10 min after the start of internalization, indicating that there is not a long lag before TacTGN38 is delivered to the TGN. We did not observe significant accumulation of TacTGN38 in late endosomes before entry into the TGN, indicating that little of the traffic goes by this route, or the passage through the late endosomes is too brief to allow detection. The simplest explanation would be direct delivery from the ERC to the TGN. The possibility of direct trafficking between the ERC and the TGN is suggested by the association of Rab11 with both the TGN and the ERC (45, 46). If TacTGN38 is directly delivered to the TGN from the ERC while Tf is recycled back to the plasma membrane, it implies that the ERC acts as a sorting site. This observation adds to our knowledge of the sorting functions of the ERC. For example, certain recycling constituents are delivered to the cell surface unimpeded while the recycling of other proteins are simultaneously slowed (28, 38). Also, some Tf trafficks in a retrograde direction from the ERC to sorting endosomes rather than recycling back to the plasma membrane (10).

We measured the rate of accumulation of anti-Tac labeled TacTGN38 in the TGN (Fig. 10) and the rate of exit of TacTGN38 on the way to the cell surface (Fig. 11). Since the amount of TacTGN38 in the TGN is at steady-state, the rate of accumulation should balance the rate of exit, which was confirmed by the independent determinations of the two rate constants that yielded the same value ($t_{1/2}$ of 46 min; Table I). The rate of accumulation of anti-TacTGN38 in the TGN and the rate of exit from the TGN are relatively slow compared with all the other steps in the trafficking of TacTGN38. The slow exit from the TGN is the major determinant of the distribution of TacTGN38.

Given the rate constants for internalization, exit from the recycling compartment, exit from the TGN, and a measurement of the amount on the surface at steady state, we can construct a simple kinetic model that allows us to predict the amount of TacTGN38 we expect to find in the TGN. In such a model, we assume the intracellular TacTGN38, C, is equal to the amount in endosomes, E, plus the amount in the TGN, T. P represents the amount on the plasma membrane that we have measured to be 11% of the total cellular amount. We can set the total cell-associated TacTGN38 as: $P + E + T = 1$. The rate of change of C is equal to the sum of the rates of change of E and T, and is given by:

$$\frac{dC}{dt} = \frac{dT}{dt} + \frac{dE}{dt}$$

$$\frac{dT}{dt} = k_{ET}(1-f)E - k_T T$$

$$\frac{dE}{dt} = k_i P - k_E f E - k_{ET}(1-f)E$$

where k_i is the internalization rate constant (0.154 min^{-1}), k_T is the rate constant for TacTGN38 delivery from the TGN to the cell surface (0.015 min^{-1}), k_E is the rate constant for TacTGN38 recycling from the recycling compartment (0.073 min^{-1}), k_{ET} is the rate of delivery from endosomes to the TGN, and f is the fraction of the internalized TacTGN38 that is recycled from the endosomes (0.82).

At steady-state, $dC/dT = 0$, and solving the above equations allows us to predict the steady-state intracellular distribution of TacTGN38. This model predicts that 82% of the total cellular TacTGN38 is in the TGN, and 7% is in endosomes (Table II). The prediction that most of the TacTGN38 is in the TGN is in agreement with the steady-

Table II. Cellular Distribution of TacTGN38

Organelle	Method of determination	% of total cellular TacTGN38
		%
Plasma membrane	Surface [^{125}I] IgG vs. total cellular [^{125}I] IgG accumulated to steady-state	11
TGN	Prediction from trafficking rate constants	82
Endosomes	Prediction from trafficking rate constants	7

state anti-Tac labeling pattern. This steady-state localization demonstrates that the apparently low efficiency of delivery of endocytosed TacTGN38 to the TGN (18% with each pass) is sufficient to accumulate the protein in the TGN. We estimate that 100,000 copies of TacTGN38 are in endosomes at steady state (7% of 1.5×10^6), which is similar to the amount of Tf receptor in the endosomes of TRVb1 cells (30).

In summary, we find that the majority of endocytosed TacTGN38 trafficks through the recycling compartment, and most of it returns to the plasma membrane on each endocytic pass. Although we cannot totally rule out the role of late endosomes as an intermediate in the postendocytic delivery of TacTGN38 to the TGN, it seems likely that the major delivery is via the ERC. TacTGN38 rapidly appears in the TGN, and slowly goes from the TGN to the plasma membrane. A simple, first-order trafficking scheme can account for the predominant distribution of TacTGN38 in the TGN.

We are grateful to Dr. Juan Bonifacino for supplying us with the TacTGN38 construct, Dr. Keith Stanley for the antibodies against TGN38's cytoplasmic domain, Dr. Yukio Ikehara for the anti-furin antibodies, and Dr. Amy Johnson for her help in isolating single clones of TRVb1 cells expressing TacTGN38.

This work was supported by National Institutes of Health grant DK27083. W.G. Mallet was supported by a fellowship from the Pharmaceutical Research and Manufacturers of America.

Received for publication 5 May 1998 and in revised form 13 July 1998.

References

1. Banting, G., and S. Ponnambalam. 1997. TGN38 and its orthologues: roles in post-TGN vesicle formation and maintenance of TGN morphology. *Biochim. Biophys. Acta*. 1355:209–217.
2. Besterman, J.M., J.A. Airhart, R.C. Woodworth, and R.B. Low. 1981. Exocytosis of pinocytosed fluid in cultured cells: kinetic evidence for rapid turnover and compartmentation. *J. Cell Biol*. 91:716–727.
3. Bos, K., C. Wraight, and K.K. Stanley. 1993. TGN38 is maintained in the *trans*-Golgi network by a tyrosine-containing motif in the cytoplasmic domain. *EMBO (Eur. Mol. Biol. Organ.) J*. 12:2219–2228.
4. Bosshart, H., J. Humphrey, E. Deignan, J. Davidson, J. Drazba, L. Yuan, V. Oorschot, P.J. Peters, and J.S. Bonifacino. 1994. The cytoplasmic domain mediates localization of furin to the trans-Golgi network en route to the endosomal/lysosomal system. *J. Cell Biol*. 126:1157–1172.
5. Dunn, K.W., and F.R. Maxfield. 1992. Delivery of ligands from sorting endosomes to late endosomes occurs by maturation of sorting endosomes. *J. Cell Biol*. 117:301–310.
6. Dunn, K.W., T.E. McGraw, and F.R. Maxfield. 1989. Iterative fractionation of recycling receptors from lysosomally destined ligands in an early sorting endosome. *J. Cell Biol*. 109:3303–3314.
7. Farquhar, M.G. 1983. Multiple pathways of exocytosis, endocytosis, and membrane recycling: validation of a Golgi route. *Fed. Proc*. 42:2407–2413.
8. Felder, S., J. LaVin, A. Ullrich, and J. Schlessinger. 1992. Kinetics of binding, endocytosis, and recycling of EGF receptor mutants. *J. Cell Biol*. 117: 203–212.
9. Ghosh, R.N., D.L. Gelman, and F.R. Maxfield. 1994. Quantification of low density lipoprotein and transferrin endocytic sorting in HEp2 cells using confocal microscopy. *J. Cell Sci*. 107:2177–2189.
10. Ghosh, R.N., and F.R. Maxfield. 1995. Evidence for nonvectorial, retrograde transferrin trafficking in the early endosomes of HEp2 cells. *J. Cell Biol*. 128:549–561.
11. Green, S.A., and R.B. Kelly. 1992. Low density lipoprotein receptor and cation-independent mannose 6-phosphate receptor are transported from the cell surface to the Golgi apparatus at equal rates in PC12 cells. *J. Cell Biol*. 117:47–55.
12. Gruenberg, J., and F.R. Maxfield. 1995. Membrane transport in the endocytic pathway. *Curr. Opin. Cell Biol*. 7:552–563.
13. Holthuis, J.C.M., B.J. Nichols, S. Dhruvakumar, and H.R.B. Pelham. 1998. Two syntaxin homologues in the TGN/endosomal system of yeast. *EMBO (Eur. Mol. Biol. Organ.) J*. 17:113–126.
14. Honegger, A.M., T.J. Dull, S. Felder, E. Van Obberghen, F. Bellot, D. Szapary, A. Schmidt, A. Ullrich, and J. Schlessinger. 1987. Point mutation at the ATP binding site of EGF receptor abolishes protein-tyrosine kinase activity and alters cellular routing. *Cell*. 51:199–209.
15. Humphrey, J.S., P.J. Peters, L.C. Yuan, and J.S. Bonifacino. 1993. Localization of TGN38 to the trans-Golgi network: involvement of a cytoplasmic tyrosine containing sequence. *J. Cell Biol*. 120:1123–1135.
16. James, D.E., R.C. Piper, and J.W. Slot. 1994. Insulin stimulation of GLUT-4 translocation: a model for regulated recycling. *Trends Cell Biol*. 4:120–126.
17. Jin, M., G.G. Sahagian, and M.D. Snider. 1989. Transport of surface mannose 6-phosphate receptor to the Golgi complex in cultured human cells. *J. Biol. Chem*. 264:7675–7680.
18. Johnson, A.O., R.N. Ghosh, K.W. Dunn, R. Garippa, G. Park, S. Mayor, F.R. Maxfield, and T.E. McGraw. 1996. Transferrin receptor containing the SDYQRL motif of TGN38 causes a reorganization of the recycling compartment but is not targeted to the TGN. *J. Cell Biol*. 135:1749–1762.
19. Johnson, K.F., and S. Kornfeld. 1992. The cytoplasmic tail of the mannose 6-phosphate/insulin-like growth factor-II receptor has two signals for lysosomal enzyme sorting in the Golgi. *J. Cell Biol*. 119:249–257.
20. Johnson, K.F., and S. Kornfeld. 1992. A His-Leu-Leu sequence near the carboxyl terminus of the cytoplasmic domain of the cation-dependent mannose 6-phosphate receptor is necessary for the lysosomal enzyme sorting function. *J. Biol. Chem*. 267:17110–17115.
21. Jones, B.G., L. Thomas, S.S. Molloy, C.D. Thulin, M.D. Fry, K.A. Walsh, and G. Thomas. 1995. Intracellular trafficking of furin is modulated by the phosphorylation state of a casein kinase II site in its cytoplasmic tail. *EMBO (Eur. Mol. Biol. Organ.) J*. 14:5869–5883.
22. Kornfeld, S. 1992. Structure and function of the mannose 6-phosphate/insulin like growth factor II receptors. *Annu. Rev. Biochem*. 61:307–330.
23. Ladinsky, M.S., and K.E. Howell. 1992. The *trans*-Golgi network can be dissected structurally and functionally from the cisternae of the Golgi complex by brefeldin A. *Eur. J. Cell Biol*. 59:92–105.
24. Ladinsky, M.S., and K.E. Howell. 1993. An electron microscopy study of TGN38/41 dynamics. *J. Cell Sci*. 17(Suppl.):41–47.
25. Lai, W.H., P.H. Cameron, I. Wada, J.J. Doherty II, D.G. Kay, B.I. Posner, and J.J. Bergeron. 1989. Ligand-mediated internalization, recycling, and downregulation of the epidermal growth factor receptor in vivo. *J. Cell Biol*. 109:2741–2749.
26. Lippincott-Schwartz, J., L. Yuan, C. Tipper, M. Amherdt, L. Orci, and R.D. Klausner. 1991. Brefeldin A's effects on endosomes, lysosomes and the TGN suggest a general mechanism for regulating organelle structure and membrane traffic. *Cell*. 67:601–616.
27. Luzio, J.P., B. Brake, G. Banting, K. Howell, P. Braghetta, and K.K. Stanley. 1990. Identification, sequencing and expression of an integral membrane protein of the *trans*-Golgi network (TGN38). *Biochem. J*. 270:97–102.
28. Marsh, E.W., P.L. Leopold, N.L. Jones, and F.R. Maxfield. 1995. Oligomerized transferrin receptors are selectively retained by a lumenal sorting signal in a long-lived endocytic recycling compartment. *J. Cell Biol*. 129:1509–1522.
29. Mayor, S., J.F. Presley, and F.R. Maxfield. 1993. Sorting of membrane components from endosomes and subsequent recycling to the cell surface occurs by a bulk flow process. *J. Cell Biol*. 121:1257–1269.

29a. Mayor, S., S. Sabharanjak, and F.R. Maxfield. 1988. Cholesterol-dependent retention of GPI-anchored proteins in endosomes. *EMBO (Eur. Mol. Biol. Organ.) J*. In press.

30. McGraw, T.E., L. Greenfield, and F.R. Maxfield. 1987. Functional expression of the human transferrin receptor cDNA in Chinese hamster ovary cells deficient in endogenous transferrin receptor. *J. Cell Biol*. 105:207–214.
31. McGraw, T.E., and F.R. Maxfield. 1990. Human transferrin receptor internalization is partially dependent upon an aromatic amino acid on the cytoplasmic domain. *Cell Regul*. 1:369–377.
32. Misumi, Y., K. Oda, T. Fujiwara, N. Takami, K. Tachiro, and Y. Ikehara. 1991. Functional expression of furin demonstrating its intracellular localization and endoprotease activity for processing of proalbumin and complement pro-C3. *J. Biol. Chem*. 266:16954–16959.
33. Molloy, S.S., L. Thomas, J.K. VanSlyke, P.E. Stenberg, and G. Thomas. 1994. Intracellular trafficking and activation of the furin proprotein convertase: localization to the TGN and recycling from the cell surface. *EMBO (Eur. Mol. Biol. Organ.) J*. 13:18–33.
34. Mukherjee, S., R.N. Ghosh, and F.R. Maxfield. 1997. Endocytosis. *Physiol. Rev*. 77:759–803.
35. Opresko, L.K., C.P. Chang, B.H. Will, P.M. Burke, G.N. Gill, and H.S. Wiley. 1995. Endocytosis and lysosomal targeting of epidermal growth factor receptors are mediated by distinct sequences independent of the tyrosine kinase domain. *J. Biol. Chem*. 270:4325–4333.
36. Pagano, R.E., M.A. Sepanski, and O.C. Martin. 1989. Molecular trapping of a fluorescent ceramide analogue at the Golgi apparatus of fixed cells: interaction with endogenous lipids provides a trans-Golgi marker for both light and electron microscopy. *J. Cell Biol*. 109:2067–2079.
37. Ponnambalam, S., C. Rabouille, J.P. Luzio, T. Nilsson, and G. Warren. 1994. The TGN38 glycoprotein contains two non-overlapping signals that mediate localization to the trans-Golgi network. *J. Cell Biol*. 125:253–268.
38. Presley, J.F., S. Mayor, K.W. Dunn, L.S. Johnson, T.E. McGraw, and F.R. Maxfield. 1993. The End2 mutation in CHO cells slows the rate of exit of transferrin receptors from the recycling compartment but bulk membrane recycling is unaffected. *J. Cell Biol*. 122:1231–1241.
39. Rajasekaran, A.K., J.S. Humphrey, M. Wagner, G. Miesenbock, A.L. Bivic, J.S. Bonifacino, and E. Rodriguez-Boulan. 1994. TGN38 recycles

basolaterally in polarized Madin-Darby canine kidney cells. *Mol. Biol. Cell*. 5:1093–1103.
40. Reaves, B., M. Horn, and G. Banting. 1993. TGN38/41 recycles between the cell surface and the TGN: Brefeldin A affects its rate of return to the TGN. *Mol. Biol. Cell*. 4:93–105.
41. Salzman, N.H., and F.R. Maxfield. 1988. Intracellular fusion of sequentially formed endocytic compartments. *J. Cell Biol*. 106:1083–1091.
42. Salzman, N.H., and F.R. Maxfield. 1989. Fusion accessibility of endocytic compartments along the recycling and lysosomal endocytic pathway in intact cells. *J. Cell Biol*. 109:2097–2104.
43. Snider, M.D., and O.C. Rogers. 1985. Intracellular movement of cell surface receptors after endocytosis: resialylation of asialo-transferrin receptor in human erythroleukemia cells. *J. Cell Biol*. 100:826–834.
44. Stanley, K.K., and K.E. Howell. 1993. TGN38/41: a molecule on the move. *Trends Cell Biol*. 3:252–255.
45. Ullrich, O., S. Reinsch, S. Urbe, M. Zerial, and R.G. Parton. 1996. Rab11 regulates recycling through the pericentriolar recycling endosome. *J. Cell Biol*. 135:913–924.
46. Urbe, S., L.A. Huber, M. Zerial, S.A. Tooze, and R.G. Parton. 1993. Rab11, a small GTPase associated with both constitutive and regulated secretory pathways in PC12 cells. *FEBS Lett*. 334:175–182.
47. Voorhees, P., E. Deignan, E.V. Donselaar, J. Humphrey, M.S. Marks, P.J. Peters, and J.S. Bonifacino. 1995. An acidic sequence within the cytoplasmic domain of furin functions as a determinant of *trans*-Golgi network localization and internalization from the cell surface. *EMBO (Eur. Mol. Biol. Organ.) J*. 14:4961–4975.
48. Wiley, H.S., and D.D. Cunningham. 1982. The endocytotic rate constant. A cellular parameter for quantitating receptor-mediated endocytosis. *J. Biol. Chem*. 257:4222–4229.
49. Wong, S.H., and W. Hong. 1993. The SXYQRL sequence in the cytoplasmic domain of TGN38 plays a major role in *trans*-Golgi network localization. *J. Biol. Chem*. 268:22853–22862.
50. Wood, S.A., J.E. Park, and W.J. Brown. 1991. Brefeldin A causes a microtubule-mediated fusion of the *trans*-Golgi network and early endosomes. *Cell*. 67:591–600.
51. Yamashiro, D.J., B. Tycko, S.R. Fluss, and F.R. Maxfield. 1984. Segregation of transferrin to a mildly acidic (pH 6.5) para-golgi compartment in the recycling pathway. *Cell*. 37:789–800.